ACS OMEGA

Open Access

http://pubs.acs.org/journal/acsodf

Article

A Fluorescent Protein-Tagged Scorpion Toxin with Picomolar Affinity for the Kv1.3 K^+ Channel

Jesús Borrego,[‖] Muhammad Umair Naseem,[‖] Amna Al Olaimi, Eva Korpos, Arpad Szoor, Gyula Batta, and Gyorgy Panyi*

Cite This: https://doi.org/10.1021/acsomega.5c10479

Read Online

ACCESS | Metrics & More | Article Recommendations | Supporting Information

ABSTRACT: The fusion of fluorophores and peptide pore blockers generates valuable molecular tools to identify cells that express the voltage-gated potassium channel Kv1.3. Changes in the Kv1.3 expression are associated with numerous autoimmune and neurological disorders. In this study, Vm24, a potent and selective Kv1.3 inhibitor peptide isolated from scorpion venom, was genetically linked to mCherry, a red fluorescent protein characterized by high photostability, maturation, and tagging tolerance. The recombinant fusion protein (mCherry-Vm24) was expressed utilizing the *Pichia pastoris* expression system. Following protein purification using affinity chromatography and size-exclusion HPLC, the production of the correct fusion-peptide was confirmed using native PAGE, mass spectrometry, spectrophotometry, and electrophysiology. mCherry-Vm24 showed ~90-fold lower, albeit still picomolar (K_d = 280 pM), affinity for Kv1.3 as compared the native Vm24, but retained its high Kv1.3 selectivity and practically irreversible binding to Kv1.3. Confocal microscopy and flow cytometry reported that CHO cells expressing hKv1.3 channels were specifically labeled with mCherry-Vm24. Biodistribution of the fusion protein in mice showed the highest fluorescence signal in the kidneys and a specific increase of the mCherry-Vm24 signal in the spleen over nonconjugated mCherry. These unique properties make the mCherry-Vm24 construct suitable for visualization of Kv1.3 both in vitro and in vivo.

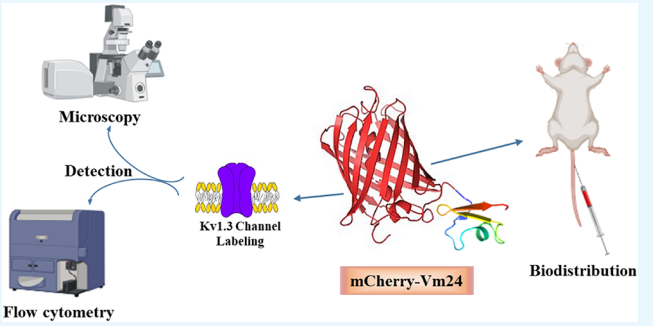

INTRODUCTION

Kv1.3 is a voltage-gated K^+ channel belonging to the *Shaker*-related subfamily (Kv1, KCNA3).[1] Kv1.3 controls the membrane potential in T lymphocytes, which is critical for the activation of these immune cells.[2] Moreover, it has been shown that Kv1.3 is highly expressed in macrophages, microglia, and effector memory cells (T_{EM} cells), suggesting that Kv1.3 plays a crucial role in immune and inflammatory responses to several human diseases,[3] where the expression of this channel is significantly elevated.[4] Kv1.3 is also expressed in nonimmune cells in pathological states, such as vascular smooth muscle cells,[5,6] and in a range of cancer cells.[7] Several techniques allow the study of the Kv1.3 channel in cells. The patch-clamp technique is widely used to determine functional Kv1.3 channels in the cells, but requires highly specialized equipment and is time-consuming. Reverse transcriptase-PCR and Western blot provide evidence of the channel transcript or protein expression, but not the number of functional channels in the cell membrane.[8] Another option for studying this channel is to use Kv1.3-specific antibodies. Antibodies that target intracellular epitopes require cell permeabilization before use. Conversely, antibodies that bind to extracellular loops can achieve good selectivity for Kv1.3 over other Kv1 subunits. However, they cannot readily distinguish between folded and unfolded channels or homotetrameric and heterotetrameric channels.[9] Numerous blockers have been utilized to investigate the structure and function of the Kv1.3 channel. These blockers include small organic molecules and peptide toxins that have been isolated from animal venoms. While small molecules exhibit affinity in the range of nM and display modest selectivity,[7] peptide toxins exhibit picomolar affinity and selectivity of several orders of magnitude over the Kv1 channels.[10] Biological imaging enables the visualization of structure and function in unperturbed environments using fluorescence markers and reporter proteins. This allows for the observation of dynamic processes in real-time, from macroscopic to subcellular and molecular levels, both in vitro and in vivo.[11] Peptides that directly block the Kv1.3 channel pore, labeled with fluorescent molecules, can be used as powerful tools for this technique. These ligands can be produced either by chemically conjugating the peptide blockers with

Received: October 8, 2025
Revised: January 29, 2026
Accepted: February 4, 2026

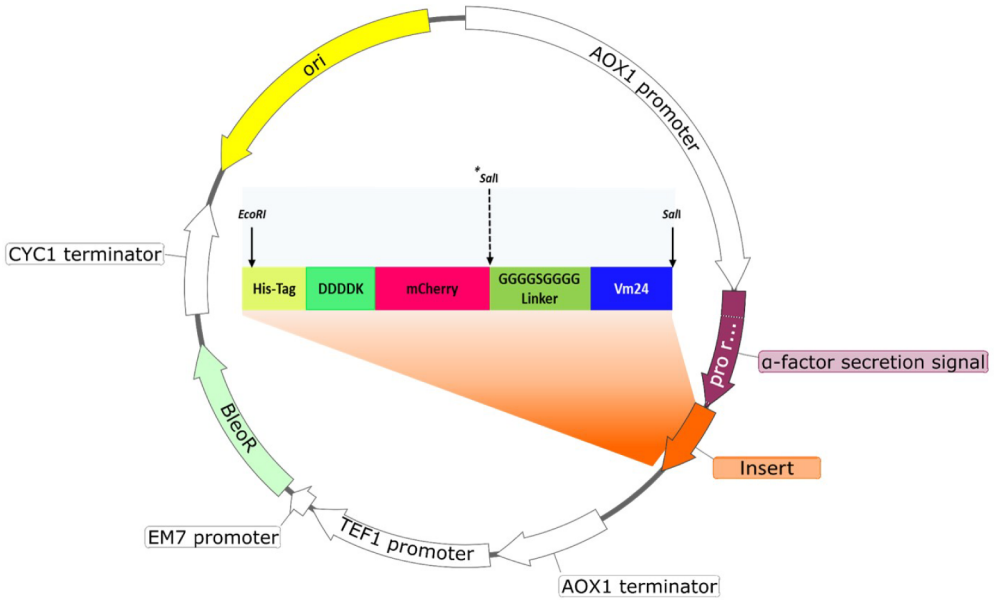

Figure 1. Schematic diagram representing the recombinant plasmids pPICZαA-mCherry-Vm24 and pPICZαA-mCherry. The insert consists of the 6× His-tag, the enterokinase protease site, the mCherry gene, a glycine-serine-glycine linker, and the Vm24 gene. The dash arrow represents the C-terminus for the plasmid pPICZαA-mCherry. The pPICZαA-mCherry construct lacks the GS linker and Vm24.

fluorescent organic dyes, some examples of these probes are ShK-F6CA,[8] HgTx1-Cy5,[12,13] HsTx1-Cy5,[12] and AgTx-2-TAMRA,[14] or by fusing the target peptides with fluorescent proteins by bioengineering methods giving molecules such as AgTx-2-RFP,[15] AgTx-2-GFP,[16] OSK1-eGFP,[15] HgTx1-RFP,[17] and MgTx-GFP.[18] All of these fluorescent-labeled peptides exhibit varying affinities toward the Kv1.3 channel, ranging from picomolar to nanomolar. Additionally, their selectivity toward other Kv1 channels may differ. In some cases, it has been observed that the fusion protein binds not only to the Kv1.3 channel but also to the Kv1.1[15,17] and Kv1.6 channels.[15] Moreover, the properties of the conjugated fluorescent proteins (i.e., GFP) confer limited in vivo applicability to the fusion proteins.[19] Therefore, it is necessary to develop molecules with higher affinity and selectivity and combine them with tags having better properties for in vivo imaging. In this study, Vm24, a potent (K_d = 3 pM) and selective Kv1.3 inhibitor peptide isolated from the scorpion *Vaejovis mexicanus smithi* venom, with an almost irreversible binding to the channel,[20] was genetically linked to mCherry, a red fluorescent protein characterized by high photostability, maturation and tagging tolerance.[21] The resulting recombinant protein was expressed utilizing the *Pichia pastoris* expression system, and its potential as a visualization tool for the Kv1.3 channel was evaluated.

RESULTS AND DISCUSSION

Design and Properties of mCherry-Vm24

The fusion protein gene was constructed by combining the coding sequences of Vm24 and the mCherry protein. Vm24 was selected for its well-documented efficacy in blocking the Kv1.3 channel with high selectivity, as well as its extensive characterization by our research group and others.[20,22,23] On the other hand, it is well established that mammalian tissues exhibit strong absorption of visible light below 600 nm due to the presence of hemoglobin.[24] Consequently, the use of fluorescent proteins with red fluorescent emission profiles can be advantageous, as these wavelengths can penetrate biological tissues with greater ease than shorter wavelengths,[25,26] which confers an advantage over proteins such as the green fluorescent protein (GFP). As a result, mCherry was selected for its red fluorescent emission profile. Three additional features were added to the fusion protein: a His-tag, an enterokinase protease site (DDDDK), and the GS linker (GGGGSGGGGG). The His-tag was added to facilitate the extraction of mCherry-Vm24 from the culture supernatant by affinity chromatography, thereby simplifying protein purification. To generalize the cloning strategy for peptide-fluorophore conjugates, an enterokinase protease site was also added between the His-tag and the mCherry protein to allow the removal of the His-tag if the presence of the His-tag negatively influences the interaction of the construct with the Kv1.3 channel.[22] Enterokinase cleavage was not applied for the mCherry-Vm24 construct in this study, as we have shown earlier that the His-tag does not influence the pharmacological properties of Vm24. The GS flexible linker was added to provide flexibility and allow motional freedom of the connecting functional proteins. The Ser in the middle maintains the stability of the linker in aqueous solutions by forming hydrogen bonds with the water molecules, thereby reducing the unfavorable interaction between the linker and the protein moieties.[27] Following the PCR and cloning procedures, the plasmids pPICZαA-mCherry-Vm24 and pPICZαA-mCherry were produced (Figure 1). Analysis of the nucleotide sequences confirmed the in-frame ligation and the expected DNA sequence encoding the recombinant proteins.

The linearized plasmid was used to transform *P. pastoris* X-33 competent cells, resulting in approximately 40 colonies. Twenty-five colonies were selected to test their hyperresistance to Zeocin. Nine colonies that showed the best growth at 2000 μg/mL of Zeocin were used to evaluate protein expression. Figure 2 shows the tricine SDS-PAGE, confirming the expression of mCherry-Vm24 with a band above 30 kDa in the gel. The band is at the predicted molecular mass range,

https://doi.org/10.1021/acsomega.5c10479
ACS Omega XXXX, XXX, XXX−XXX

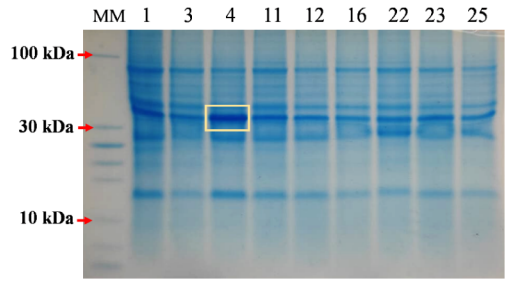

Figure 2. Tricine SDS-PAGE analysis of mCherry-Vm24 recombinant expression. The culture supernatant of 9 clones grown at 2000 μg/mL zeocin concentration was analyzed using 16% tricine SDS-PAGE. Line MM is the molecular marker (kDa). The numbers above each sample represent the chosen clone. The yellow square highlights the selected clone with the highest expression of the recombinant mCherry-Vm24 construct.

considering the 32 kDa molecular mass of the conjugate (see below). Colony 4 gave the largest production yield and thus was chosen to produce recombinant mCherry-Vm24 in a 50 mL culture. After confirming proper protein expression, the culture was scaled up to 1 L. The eluted protein from the Nickel-NTA affinity chromatography and size-exclusion high-performance liquid chromatography (SE-HPLC) exhibited a fuchsia color that turned dark purple when it was concentrated due to the presence of the mCherry protein (Figure S1), the same color previously reported.[28]

Initially, the fusion protein was attempted to be purified with reversed-phase high-performance liquid chromatography (RP-HPLC). However, the protein lost its fuchsia color and turned yellow, showing aggregates under the microscope (data not shown). Some fluorescent proteins are sensitive to changes in pH, which can result in a loss of brightness and result in oligomerization.[29,30] This effect was most likely caused by the acidic conditions of the solutions used in the RP-HPLC. Based on our observation, it is important to note that RP-HPLC is not suitable for purifying the mCherry-tagged peptide and, therefore, SE-HPLC was used instead. Figure 3A shows the chromatogram obtained from the SE-HPLC, which resulted in three main fractions (F1, F2, and F3) with retention times of 11.4, 12.8, and 14.1 min, respectively, and a total yield of 5.9 mg/L. To evaluate the traits of the fractions and determine if they could be used interchangeably, the fractions were run on a 16% native PAGE, and all showed a band with a reddish fluorescent signal under blue light from a transilluminator (Figure 3B), confirming that all bands contain the fluorophore. To determine the functional properties of F1−F3 peptides, patch-clamp was used, and we measured the block of the whole-cell Kv1.3 current in the presence of each of the fractions separately. Figure 3C shows that only F3 blocked

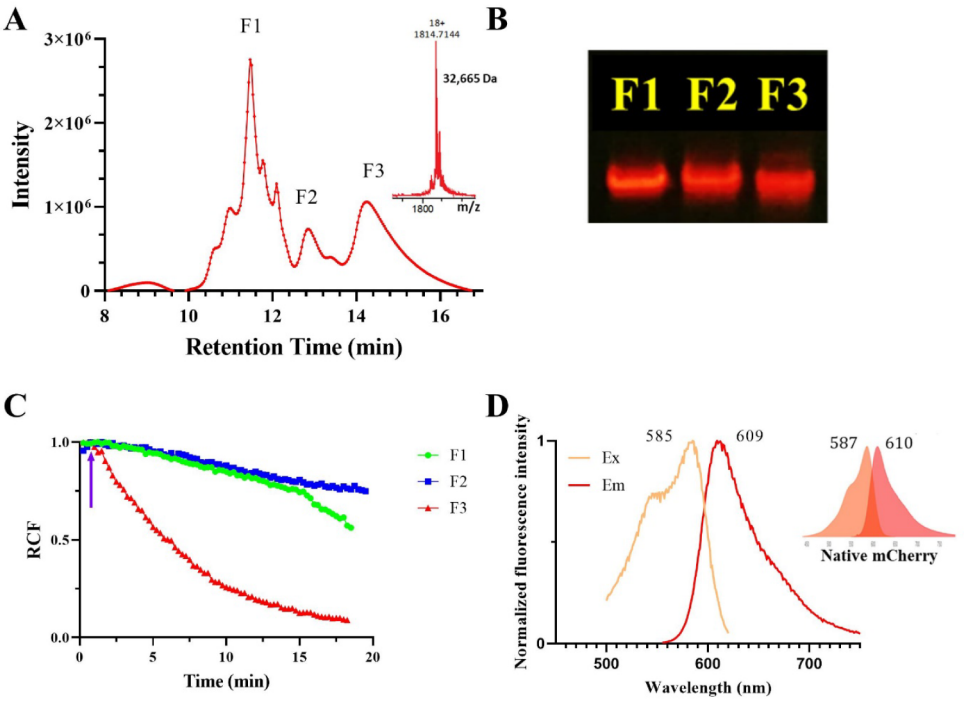

Figure 3. Characterization of recombinant mCherry-Vm24. (A) Concentrated eluate from affinity chromatography was loaded on the SEC column, and absorption at 280 nm was measured and plotted as a function of time. Three main fractions were obtained after SE-HPLC purification (F1: fraction 1, F2: fraction 2, and F3: fraction 3). The inset in the chromatogram represents an ESI-QTOF-MS spectrum showing the average mass of fraction 3. (B) Fluorescence image of the mCherry bands (transilluminator blue light excitation) F1, F2, and F3 in a 16% native PAGE. (C) Each of the fractions (F1−F3) was tested individually at 1 nM concentration on the hKv1.3 current measured in human peripheral T lymphocytes. Peak currents (I), measured in the presence of 1 nM concentration of F1−F3 at +50 mV, were normalized to the current measured in the absence of the mCherry-Vm24 (I_0) to get RCF = I/I_0, and plotted as a function of time. The holding potential was −120 mV, depolarizing pulses were delivered every 15 s. The perfusion of the recording chamber with 1 nM Fraction 1 (F1, green dots), Fraction 2 (F2, blue squares), and Fraction 3 (F3, red up triangles) started as indicated by the purple arrow. (D) Fluorescence excitation (Ex, yellow) and emission (Em, red) spectra of fraction 3 measured in a spectrofluorometer (see Methods). The fluorescence intensities were normalized to the maxima to give values on the y-axis. Numbers to the left and right of the spectra indicate the maxima in nm. The inset shows the schematic excitation and emission spectra for native mCherry.[29]

https://doi.org/10.1021/acsomega.5c10479
ACS Omega XXXX, XXX, XXX−XXX

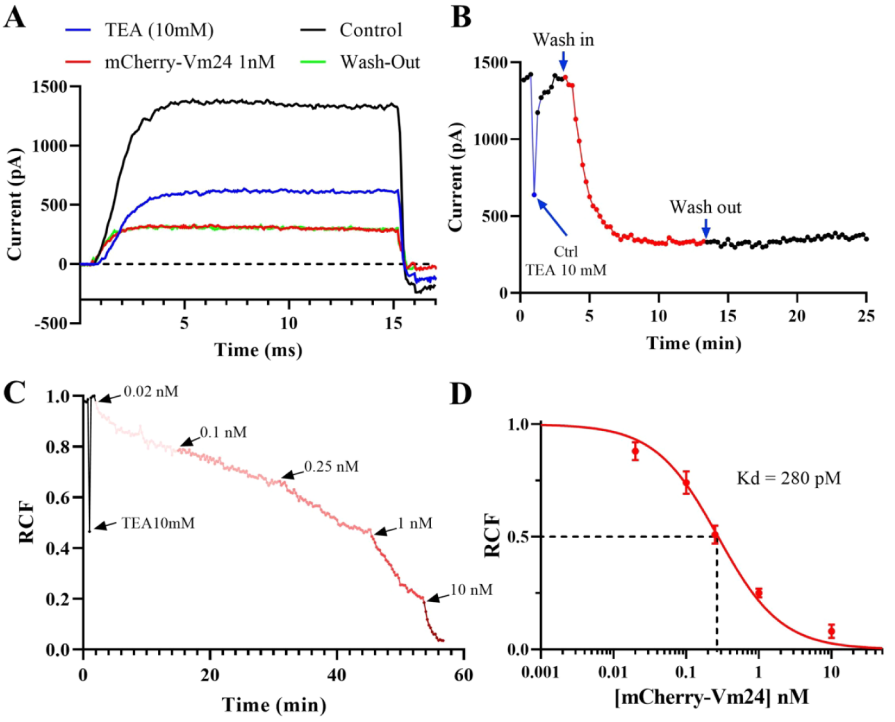

Figure 4. Electrophysiological characterization of recombinant mCherry-Vm24 on the hKv1.3 channel. (A) Activated human peripheral T lymphocytes were depolarized to +50 mV from a holding potential of −120 mV for 15 ms to elicit whole-cell currents mediated by hKv1.3. Test pulses were applied every 15 s. Representative trace shows the K^+ current in the absence of mCherry-Vm24 (control, black trace), after reaching the equilibrium block in the presence of mCherry-Vm24 (red trace), and after the perfusion of free-toxin extracellular solution after the equilibrium block (wash-out, green). The proper operation of extracellular solution exchange in the recording chamber was assured by testing the fully reversible inhibitor TEA (10 mM, blue trace). (B) The time course of the inhibition of the peak hKv1.3 currents is shown. The peak currents were determined in the absence (black dots) and in the presence of mCherry-Vm24 (red dots) and plotted as a function of time. Arrows indicate the start (wash-in) and end (wash-out) of the perfusion with 1 nM mCherry-Vm24. The perfusion of the recording chamber with TEA served as a positive control for perfusion (blue dot). (C) Recombinant mCherry-Vm24 blocked hKv1.3 in a concentration-dependent manner. The time course of the hKv1.3 remaining current fraction (RCF) following the administration of increasing concentrations of mCherry-Vm24 (0.02−10 nM) is represented by different red shade dots, and the start of the perfusion is indicated by arrows. (D) The average remaining current fraction (RCF, I/I_0) values were calculated at different toxin concentrations, and a Hill equation (see Materials and Methods for details) was fitted to the data points. The best fit was obtained with Hill coefficient = 0.82 and K_d = 280 pM. n = 3−4. The dashed line indicates the concentration at which 50% of the current remains in the presence of mCherry-Vm24. Error bars indicate mean ± SEM.

Kv1.3 with block kinetics similar to those observed in the synthetic and recombinant versions of Vm24.[20,22] Protein expression and purification processes may result in the aggregation of the recombinant protein. However, these aggregates can be removed using SEC, as they have a different shape and molecular weight than the desired protein, appearing at shorter retention times.[31,32] F1 and F2 were likely mCherry-Vm24 aggregates, where the fluorescence of mCherry was not affected but the interaction of Vm24 with Kv1.3 was hindered by the aggregation. Therefore, all subsequent results were obtained using fraction F3, which will be referred to as mCherry-Vm24. Although the native PAGE showed that the mCherry-Vm24 emitted fluorescence, its spectral properties were evaluated and confirmed by comparing them to those of native mCherry profiles. Figure 3D shows the excitation and emission profiles obtained for the fusion protein, with an excitation peak at 585 nm and an emission peak at 609 nm, similar to those previously reported for mCherry.[28] The molecular mass of the recombinant mCherry-Vm24 was determined using ESI QTOF-MS, giving an average mass of 32.6 kDa (Figure 3A, inset), which is in agreement with the expected mass of 32.6 kDa. The same protocols were employed for the expression and purification of the mCherry protein (Figure S1). The mCherry protein yield was 12.4 mg/L, with an average mass of 29.2 kDa, which is consistent with the expected mass of 29.2 kDa. Furthermore, the recombinant mCherry protein displayed red fluorescence under blue light, as anticipated (Figure S1). The recombinant mCherry protein was employed as a control in the biodistribution experiments.

Electrophysiological Characterization of mCherry-Vm24

Three sets of experiments were conducted to compare the characteristics of mCherry-Vm24 with those of Vm24 peptides previously reported either in its native, synthetic, or recombinant version, i.e., block kinetics, Kv1.3 affinity, and selectivity. One of the most significant features of Vm24 is that the block is practically irreversible within the usual duration of whole-cell patch-clamp experiments.[23] This property of the native Vm24 was maintained in the mCherry-Vm24 conjugate. Figure 4A shows that upon the application of 1 nM of mCherry-Vm24, the hKv1.3 current was inhibited to ∼20% of the control current obtained in the absence of Vm24. The block developed rapidly, and the peak current recovered negligibly upon perfusing the recording chamber with toxin-free extracellular solution applied for more than 10 min (Figure 4B). This suggests that the off-rate of the toxins is very slow, and the mCherry-Vm24 remains bound to the channels

https://doi.org/10.1021/acsomega.5c10479
ACS Omega XXXX, XXX, XXX−XXX

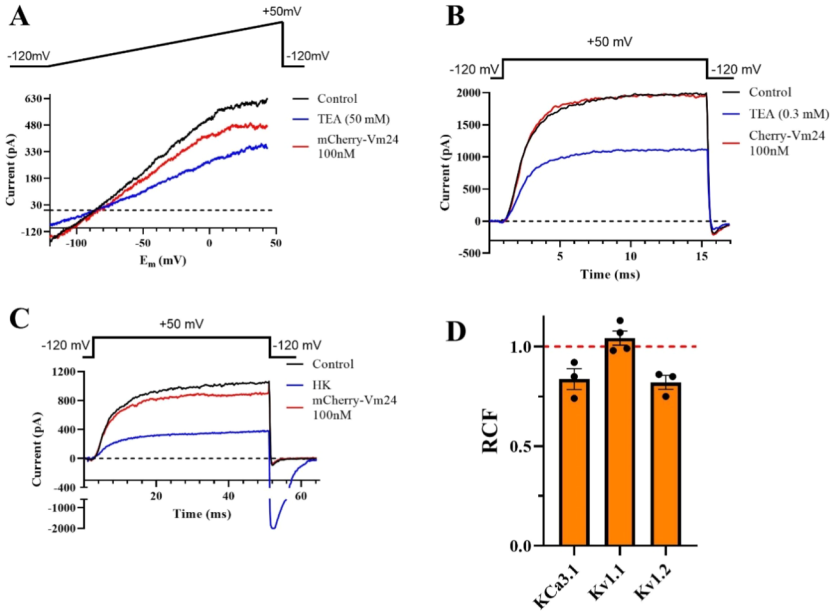

Figure 5. Selectivity profile of mCherry-Vm24. Representative current traces of hKCa3.1 (A), hKv1.1 (B), and hKv1.2 (C) channels are shown in each panel. The traces were recorded in the absence of the mCherry-Vm24 (control trace in black) and with 100 nM mCherry-Vm24 (trace in red). Recordings were taken either at equilibrium block (A and C) or after 28 depolarization pulses over 7 min. To ensure the proper operation of extracellular solution exchange in the recording chamber, the fully reversible inhibitor TEA or HK solution (HK: HK-150 solution with high extracellular (150 mM) K^+ to reduce the K^+ driving force) was tested frequently as a positive control. The voltage protocols are provided above the current traces in each panel. (D) Remaining current fraction (RCF, I/I_0) values were calculated as the ratio of the peak currents in the presence (I) or absence (I_0) of 100 nM mCherry-Vm24 at steady state block for hKCa3.1 and hKv1.2 channels or after 7 min of application of toxin to the cells expressing hKv1.1 channels. Error bars represent SEM (n = 3−4), each symbol is an independent data point.

over the reasonably long duration of the experiment. Due to the very slow off-rate of the mCherry-Vm24, a cumulative concentration−response curve was obtained for the block of hKv1.3 (Figure 4C). At concentrations >1 nM, the block developed with the predicted exponential kinetics (Figure 4B). However, the very slow development of the equilibrium block posed significant difficulties in the determination of the peak current in the presence of low mCherry-Vm24 concentrations.[20] In the presence of low (<1 nM) peptide concentrations, peak currents were determined when the current traces were superimposable in the data acquisition window of pClamp, i.e., peak currents were virtually constant. The Hill equation fitted to the remaining current fraction values (RCF, see Materials and Methods) obtained at various mCherry-Vm24 concentrations resulted in K_d = 280 pM with n_H = 0.82 (Figure 4D). The K_d of mCherry-Vm24 is 93-fold larger than the reported K_d for Vm24 (3 pM).[23] Our previous study showed that the addition of a short peptide segment (14 extra amino acid residues) to the N-terminus of recombinant Vm24 does not significantly affect its interaction with the Kv1.3 channel.[22] However, the K_d of the mCherry-Vm24 fusion protein was slightly decreased due to the addition of mCherry. A similar decrease in the affinity of RFP-HgTx1 was also observed with a K_d value of 15 ± 3 nM,[17] 177-fold higher than the K_d of the nonfusion HgTx1 (86 pM).[33] In contrast, GFP-MgTx binds to Kv1.3 with a K_d of 11 nM, whereas nonconjugated MgTx binds with a K_d of 11 pM, indicating a 1000-fold decrease in the K_d.[18] On the other hand, when comparing the K_d values of OSK1 and AgTx2 toxins (6 ± 2 and 9 ± 2 nM, respectively) with the K_d values of their fusion counterparts, eGFP-OSK1, and RFP-AgTx2 (8 ± 2 and 83 ± 13 nM, respectively), a barely noticeable change in K_d values was observed (1.3-fold and 13.8-fold, respectively).[15] Based on these, the effect of the interaction between the fusion protein and the Kv1.3 channel is highly dependent on the properties of each fluorescent fusion peptide. In all cases, except for Vm24, the fusion proteins are characterized by K_d values in the nanomolar range. Vm24, on the other hand, maintains its blocking potency on the Kv1.3 channel at picomolar ranges despite being fused with mCherry. For toxins such as Vm24, the C-terminus plays a crucial role in its interaction with Kv1 channels.[34,35] In contrast, the N-terminus does not significantly contribute to this interaction.[36] Tags can be easily added in this latter, N-terminal region, as demonstrated in the recombinant version of Vm24, which maintains the low picomolar affinity for Kv1.3 even with a His-tag in the N-terminus.[22] However, it has been reported that the fusion of fluorescent proteins to either the N-terminus or C-terminus can affect the selectivity of the fusion peptide.[16]

The selectivity of mCherry-Vm24 was evaluated in the last step of the pharmacological characterization. Our previous paper reported that at 10 nM concentration, Vm24 partially blocked the hKCa3.1, mKv1.1, and hKv1.2 channels, resulting in remaining current fraction (RCF) values of 0.59 ± 0.03, 0.80 ± 0.02, and 0.54 ± 0.08, respectively. Thus, hKCa3.1 and hKv1.2 channels were more sensitive to Vm24 than mKv1.1, whereas 7 other ion channels were not inhibited by Vm24.[20] For the current study, those ion channels for which Vm24 was the least selective were included. The mCherry-Vm24 fusion protein was tested at a concentration of 100 nM on these three channels (at ∼350-fold concentration than the K_d for Kv1.3). mCherry-Vm24 exhibited the same general behavior as Vm24 by blocking hKCa3.1 (Figure 5A) and hKv1.2 (Figure 5C) channels with RFC values of 0.84 ± 0.05 (n = 3) and 0.82 ± 0.04 (n = 3), respectively (Figure 5D). The hKCa3.1 currents (Figure 4A) were measured in response to voltage ramps, as

https://doi.org/10.1021/acsomega.5c10479
ACS Omega XXXX, XXX, XXX−XXX

hKCa3.1 is voltage independent. The channel is activated by ~1 μM Ca^{2+} concentration in the pipette filling solution.[37] The reversal potential of all control and blocked currents is ~−85 mV. This value corresponds to the K^+ equilibrium potential calculated using the Nernst equation, and thus confirms that the majority of the whole-cell current is K^+ current. Moreover, 50 mM TEA inhibited ~50% of the current in good agreement with the expected behavior of the hKCa3.1 current.[38] The hKv1.2 current was measured using a 50 ms-long depolarization to +50 mV to allow full activation of the whole-cell current (Figure 5C). A quick and readily reversible method to show the proper function of the perfusion system is the application of HK (150 mM K^+) extracellular solution that reduces the peak current and increases the tail current upon repolarization to −120 mV.[39] We did not use selective Kv1.2 blocker peptides as positive controls for perfusion due to the slow wash-in and wash-out kinetics of these peptides[40,41] as compared to the expected speed of the solution exchange. The hKv1.1 currents were measured in response to 15 ms-long depolarizations to +50 mV, which allowed full activation of the current (Figure 5B). As shown previously, 0.3 mM TEA is an ideal positive control due to the high TEA affinity of hKv1.1 and very rapid block and unblock of the channels by TEA.[41] Figure 5B,D clearly demonstrated that mCherry-Vm24 at 100 nM concentration did not have any effect on hKv1.1 (RCF 1.04 ± 0.04, n = 4).

Visualization of mCherry-Vm24 on the Cell Membrane of CHO Cells Expressing hKv1.3 Channel

To evaluate the applicability of mCherry-Vm24 as a fluorescent probe to label the Kv1.3 channel, CHO cells expressing heterologously the GFP-tagged hKv1.3 channel were treated with the fusion protein, and the labeled cells were examined using confocal microscopy. Row 1 in Figure 6 shows that after incubation with 10 nM mCherry-Vm24, the mCherry-Vm24 signal was strictly localized to the cell membrane. Although the GFP-tagged hKv1.3 signal was also detected in the cytoplasm, the colocalized signal of mCherry and GFP cannot be observed in the cytoplasm of the cell, thereby proving that mCherry-Vm24 binds to Kv1.3 on the cell surface. On the other hand, a yellow ring that is localized to the plasma membrane can be observed in the merged image (Row 1, Merge column). To confirm that the mCherry signal on the membrane was not a result of nonspecific mCherry-Kv1.3 channel interaction, the experiment was repeated using recombinant mCherry that lacked the fusion with Vm24. As shown in Figure 6, Row 2, membrane fluorescence signal in the mCherry channel was not detectable on the cell surface using the same microscopy settings as with mCherry-Vm24 (see Row 1), whereas the GFP signal reporting on Kv1.3-GFP expression is clearly visible (GFP and Merge columns of Row 2). The same result was obtained with nontransfected CHO cells treated with mCherry-Vm24, which also eliminates the possibility of nonspecific labeling of the membrane (Figure 6, Row 3). It has been reported that concentrations equal to or greater than 40 nM of GFP-AgTx2 protein and derivatives resulted in nonspecific interactions with the membrane, staining both transfected and nontransfected cells.[16] On the contrary, in preliminary experiments in this work, labeling the nontransfected cells with 100 nM mCherry-Vm24 did not label the cells with red fluorescence (data not shown). Although using a low concentration of the fluorescent fusion protein may reduce the occurrence of nonspecific interactions, nonspecific

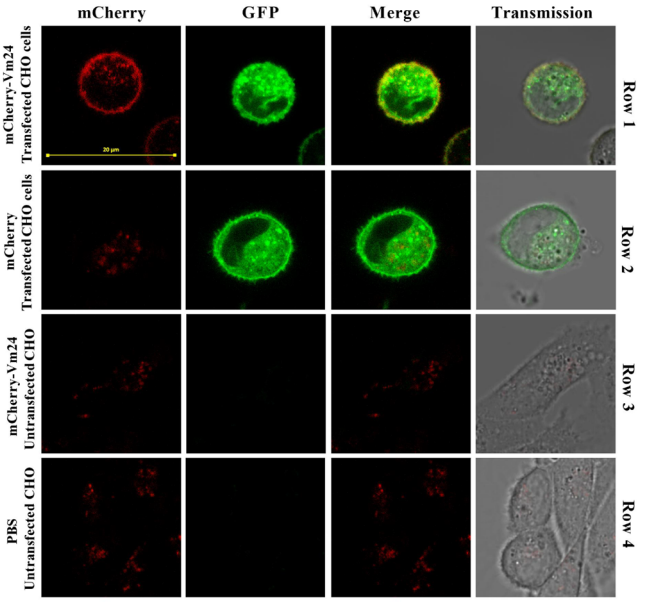

Figure 6. Confocal microscopy of CHO cells expressing GFP-tagged hKv1.3 labeled with recombinant mCherry-Vm24. Column headers: mCherry: fluorescence was detected using 543 nm excitation and 493−591 nm emission; GFP: fluorescence was detected using 488 nm excitation and 581−697 nm emission; Merge: merge of the images obtained in the mCherry and the GFP channels; Transmission: transmission image of the viewing fields are shown on the right panels. Row headers: Row 1, CHO cells expressing GFP-hKv1.3 channel after being incubated with 10 nM mCherry-Vm24 for 1 h at 37 °C. Row 2, CHO cells expressing the GFP-hKv1.3 incubated with 10 nM mCherry as above. Row 3, nontransfected CHO cells incubated with 10 nM mCherry-Vm24 as above. Row 4, nontransfected CHO cells without treatment. Experiments were repeated for three independently labeled samples, representative images are shown. The scale bar is 20 μm.

labeling at high concentrations could be characteristic of each toxin. It is noteworthy that red patchy fluorescence signals were observed in the cytoplasm of the cells in the mCherry channel. We attribute these to autofluorescence of the cells, as it is consistently detected in all experimental conditions (Figure 6, Rows 1−4), even in the simultaneous absence of the GFP-tagged Kv1.3 and the mCherry-Vm24 fusion protein (Figure 6, Row 4).

mCherry-Vm24 Can Be Used to Detect Kv1.3 Expressing CHO in Flow Cytometry

Next, we addressed whether the mCherry-Vm24 fluorescent peptide can be exploited to study Kv1.3 expression using flow cytometry. To demonstrate this, CHO cells stably expressing GFP-hKv1.3 were stained with mCherry-Vm24. The flow cytometry dot-plot of unlabeled, GFP-hKv1.3 expressing cells in Figure 7A did not show any fluorescent signal in the mCherry channel, however, more than 97% of the cells were positive for GFP (lower right quadrant). On the other hand, when GFP-hKv1.3 expressing CHO cells were stained with mCherry-Vm24 (10 nM), a substantial fraction of cells that have high hKv1.3 expression (i.e., high GFP signal) gave strong mCherry fluorescence as shown by the dot-plot in Figure 7B. In general, 88 ± 2.1% (n = 3) of the cells were positive for mCherry-Vm24 (sum of the upper quadrants), which corresponds to 91.4 ± 1.7% (n = 3) of cells that showed increased GFP signal as well (upper right quadrant over right

https://doi.org/10.1021/acsomega.5c10479
ACS Omega XXXX, XXX, XXX−XXX

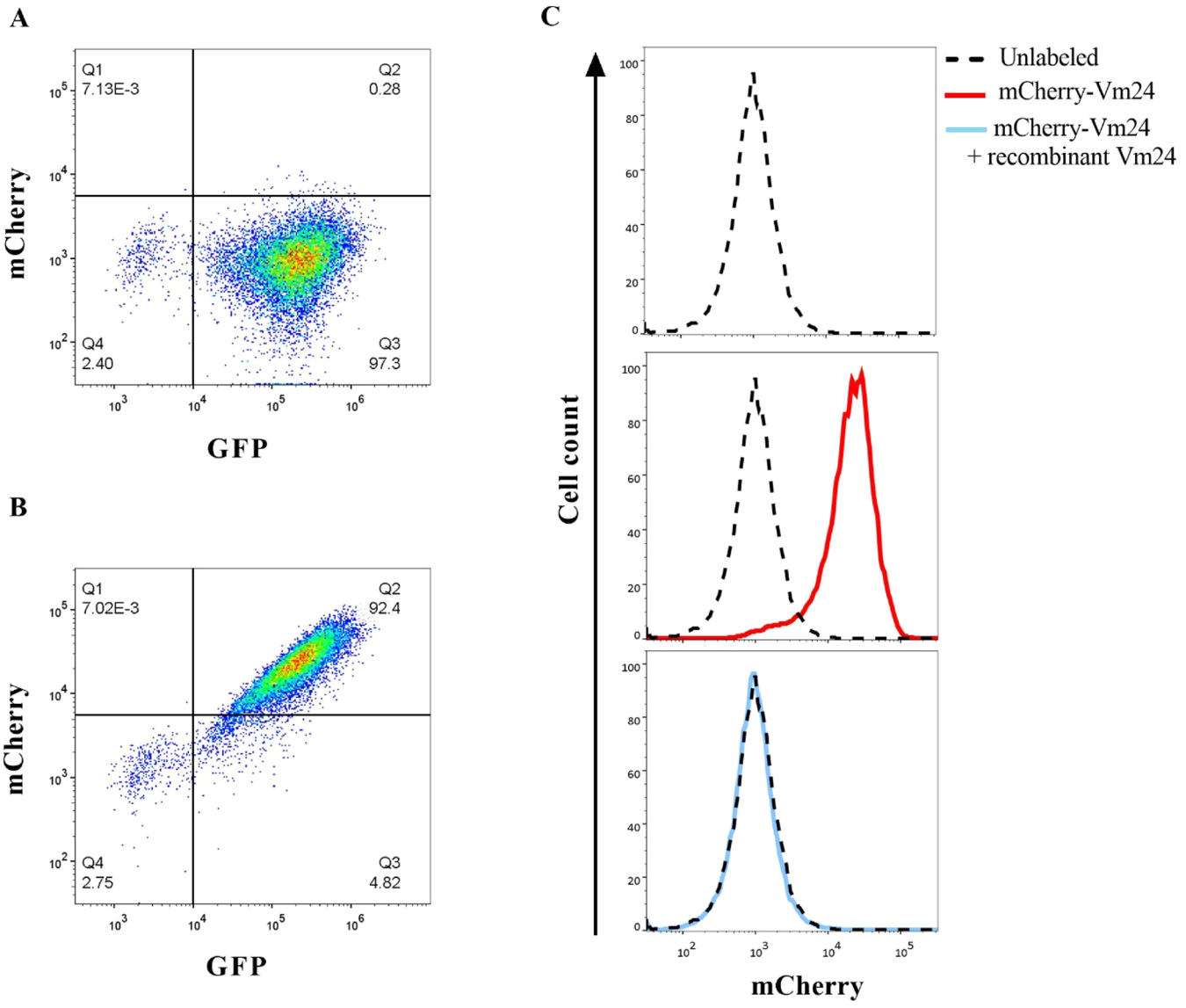

Figure 7. Detection of heterologously expressed GFP-tagged hKv1.3 channels in flow cytometry. (A–B) Representative flow cytometry dot plots of emission in the GFP (abscissa) and mCherry (ordinate) channels. The fluorescence of GFP-Kv1.3 expressing CHO cells was determined either unstained (A) or stained with 10 nM of mCherry-Vm24 (B). Values written in each quadrant show the percentage (%) of the cell population in the corresponding quadrant. (C) Fluorescence histogram of CHO cells in the mCherry channel expressing GFP-Kv1.3 without staining (top, black dashed line), stained with 10 nM of mCherry-Vm24 (middle, red line), or preincubated with 100 nM of recombinant Vm24 before staining with 10 nM of mCherry-Vm24 (bottom, blue line).

quadrants). This cell population is also represented by a right-shifted peak (in red) in the fluorescent histogram (Figure 7C). Moreover, to verify that mCherry-Vm24 specifically labels the hKv1.3-expressing cells, we carried out a competition assay. For this assay, GFP-hKv1.3 expressing CHO cells were incubated first with surplus recombinant Vm24 (rVm24, 100 nM)[22] and then stained with mCherry-Vm24. The overlaid histograms in Figure 7C demonstrate that the fluorescent histogram of CHO cells which were preincubated with surplus rVm24, can be superimposed over the control, unstained CHO population. This suggests that the rVm24 completely prevented the binding of mCherry-Vm24 to hKv1.3 channels. Other fluorescently tagged peptides that target Kv1.3 have been reported to specifically detect Kv1.3 expression both in model cells, as heterologous expression, and in primary cells, e.g., activated T cells, using flow cytometry. Previously, we have visualized the stable Kv1.3 expression in CHO cells in a flow cytometer using a cyanine5-tagged HsTX[R14A] peptide, which is a selective and potent blocker of Kv1.3.[42] Another example is a fluorescein-conjugated analog of a sea anemone toxin ShK (ShK-F6CA), which selectively inhibits the Kv1.3 currents. ShK-F6CA staining assay using a flow cytometer identified the Kv1.3 expression in chronically activated rat and human T lymphocytes,[8] microglia, and CNS-infiltrating monocytes/macrophages.[43] A fluorescently labeled toxin that targets Kv1.3 would be a useful tool in clinical diagnostics where the $Kv1.3^{high}$ T cells (e.g., activated $CD3^+$ $CCR7^-$ T_{EM} cells ~1800 Kv1.3 channels/T cells[44,45]) should be distinguished from $Kv1.3^{low}$ T cells (e.g., $CD3^+$ $CCR7^+$ naive, T_{CM}, ~200–300 Kv1.3 channels/T cells) in a flow cytometry experiment. This information may be relevant to follow the progression of T_{EM}-mediated autoimmune diseases (e.g., Multiple Sclerosis, Type1 diabetes and Rheumatoid Arthritis[44,45]), as increased Kv1.3 current density was reported

https://doi.org/10.1021/acsomega.5c10479
ACS Omega XXXX, XXX, XXX−XXX

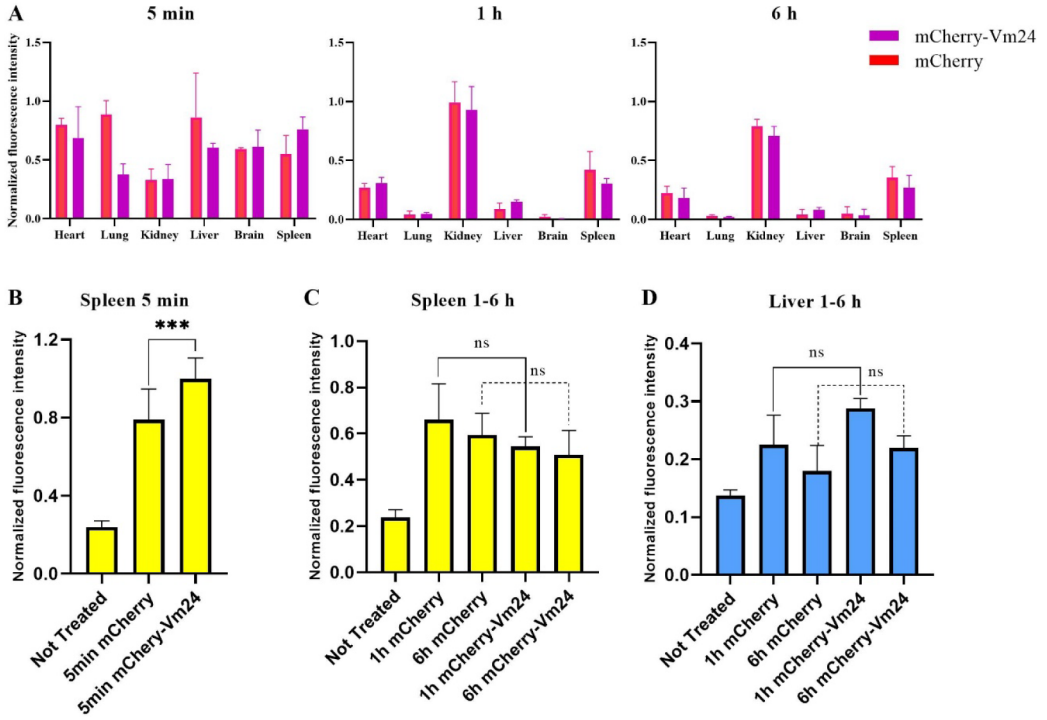

Figure 8. Quantitative analysis of fluorescence signal from mCherry-Vm24 biodistribution assay. (A) Mice were administered a dose of 3 μg/g body weight of mCherry-Vm24 or mCherry via the tail vein. At 5 min, 1 h, and 6 h postinjection, the organs were extracted and the fluorescence quantified (n = 3, mean ± SEM). To correct for background fluorescence, fluorescence readings in the indicated organs obtained from control mice, which received PBS injection, were subtracted from those obtained from the corresponding organs of mCherry- or mCherry-Vm24-injected mice. (B) Fluorescence readings in the spleen at 5 min postinjection time point in control (PBS-injected), mCherry- or mCherry-Vm24-injected animals. (C) Fluorescence readings in the spleen at 1h and 6h postinjection time points for the same groups as defined in panel B. (D) Fluorescence readings in the liver at 1h and 6h postinjection time points for the same groups as defined in panel B. (****:p < 0.0009, ns = not significant).

recently in peripheral blood T cells of MS patients.[46] Moreover, cancer cells also up-regulate Kv1.3,[47] and these cells could also be identified using mCherry-Vm24. The data presented in this paper is promising since Kv1.3 expressing CHO cells were clearly identified, however, our conclusions are limited currently to the in vitro model. Unfortunately, we were unable to show increased mCherry-Vm24 fluorescence in phytohemagglutinin-A stimulated human peripheral blood lymphocytes (data not shown). Further experimental confirmation is required for the applicability of mCherry-Vm24 to identify Kv1.3^{high} T_{EM} cells in clinical samples.

mCherry-Vm24 Biodistribution in a Mouse Model

The in vivo biodistribution of the mCherry-Vm24 fusion protein was studied by injecting mCherry-Vm24 into mice i.v. and then measuring emitted fluorescence in selected organs and comparing it to untreated controls and to those injected with recombinant mCherry lacking the Vm24 part. Measurements were taken at three distinct time points: 5 min, 1 h, and 6 h postadministration. Normalized fluorescence intensity served as the indicator of biodistribution. The analysis focused on six key organs: heart, lung, kidney, liver, brain, and spleen. The biodistribution of mCherry-Vm24 demonstrated a clear time-dependent variation in the fluorescence intensity across different organs. The highest levels were typically observed at 5 min postadministration, followed by a decline at 6 h. The exception to this trend was the kidney, which showed maximum fluorescence intensity between 1 and 6 h (Figure 8A). Similar results were observed for the biodistribution of the Cy5-HsTX1 toxin, which also binds to the Kv1.3 channel. Similar to the observation in this work, the kidney exhibited the highest Cy5-HsTX1 signal after 1 and 6 h, with a relatively poor signal coming from the other organs.[42] This unique pattern suggests prolonged retention or delayed peak of mCherry-Vm24 in renal tissues, possibly due to specific interactions or slower clearance mechanisms in the kidneys. The spleen exhibited a higher fluorescence intensity at 5 min postadministration in the mCherry-Vm24 group compared to the mCherry alone and the nontreated (control) group, indicating a rapid and significant initial distribution of mCherry-Vm24 to the spleen tissue (Figure 8B). At 1 and 6 h, the mCherry-Vm24 fluorescence intensity decreased in the spleen to ∼half as compared to the 5 min data, showing somewhat lower signals in the mCherry-Vm24-treated group compared to the mCherry control (Figure 8C). In mice, approximately 50% of lymphocytes from secondary lymphoid tissue are found in the spleen. The residence time of lymphocytes in the spleen has been estimated for different animals, with an estimated range of 4−5 h for rats,[48] 2−4 h for pigs,[49] and approximately 3 h for sheep.[50] However, using complex mathematical models, the average residence time has been calculated to be between 1.4 h[51] and 4.6 h.[48] Considering the residence time, we propose that the rapid and specific increase in the fluorescence upon mCherry-Vm24 application is due to the high concentration of immune system cells that express the Kv1.3 channel, such as T cells. This may also allow the identification of the specific cell types labeled with Vm24-mCherry either in the frozen sections of the spleen using fluorescence microscopy or flow cytometric analysis of the cells

https://doi.org/10.1021/acsomega.5c10479
ACS Omega XXXX, XXX, XXX−XXX

Table 1. Primers Used for the mCherry and mCherry-Vm24 Gene Generation[a]

Primer	Sequence
Vm24-F	5′*GGCGGTGGTGGTTCAGGCGGTGGAGGT*GCAGCTGCAATCTCCTGC3′
Vm24-R	5′CAGCTGTTAACAGTAGTAGCACTTACACTTTC3′
mCherry-F[b]	5′GAATT**CCATCACCATCACCATCACGATGATGATGATAA**GGTGAGCA AGGGCGAGGAGC3′
mCherry-R	5′*GGCGGTGGTGGTTCAGGCGGTGGAGGT*CTTGTACAGCTCGTCCATGC CGA3′
mCherry-R-*Sal*I	5′GATGGTCGACCTTGTACAGCTCGTCCATG3′

[a]The GGGSGGG linker coding sequence is presented in underlined and italicized letters. The 6×-His Tag coding sequence is presented in underlined and bold letters. [b]Primer mCherry-F was used for the construction of mCherry-Vm24 and mCherry vector.

isolated from the spleen, in combination with T cell subset specific markers. At later time points, the mCherry-Vm24 conjugate was either consumed or cleared from the spleen while being bound to the cells, which finished the residence time in the spleen.

On the other hand, mCherry-Vm24 showed a slightly, but statistically not significantly, slower clearance in the liver as compared with mCherry (Figure 8D). The liver is involved in metabolism and detoxification. It has been observed that the protein molecular weight is related to the clearance in this organ. Higher molecular weight results in greater deposition of the protein in this organ.[52] This may provide an explanation for the slight difference in signal observed at 1 and 6 h between mCherry and mCherry-Vm24. For the brain, kidney, lungs, and heart, the conjugation of Vm24 to mCherry did not cause significant tissue-specific differences in the distribution of the fluorescent protein. This suggests that mCherry-Vm24 does not preferentially accumulate in these organs or that the fluorescent marker might not adequately capture subtle distribution nuances in these tissues. In highly vascularized tissues, the movement of proteins across the vascular network, regardless of their molecular weight, may account for the observed pattern in these organs.[53] These findings align with existing literature on the biodistribution of other labeled therapeutic agents. For instance, similar patterns of rapid initial distribution followed by slower clearance have been observed with various tracers and therapeutic compounds, highlighting the importance of time-dependent dynamics in biodistribution studies.[54] Moreover, studies have shown that organs such as the liver and spleen often serve as primary sites for the accumulation and clearance of nanoparticles and other therapeutic agents, supporting the observations in this study.[55] In conclusion, the biodistribution of mCherry-Vm24 reveals important organ-specific and time-dependent dynamics that are crucial for understanding its potential therapeutic applications. These insights can inform the development of more targeted and effective delivery mechanisms for therapeutic agents, ensuring optimal distribution and efficacy while minimizing potential side effects.

EXPERIMENTAL PROCEDURES

Chemicals

All chemicals, unless stated otherwise, were purchased from Sigma-Aldrich (Budapest, Hungary).

Plasmid Construction

To construct the expression vector pPICZαA-mCherryVm24, the mCherry sequence was amplified from the vector pmCherry-Kv1.3[56] and Vm24 from the vector pPICZαA-Vm24[22] using PCR. DNA fragments were amplified using 1 U of high-fidelity Phusion polymerase by adding 10 pM primers (primers are shown in Table 1) supplemented with 1x reaction buffer, 10 mM dNTPs, and 100 ng of template DNA in a 50 μL reaction mixture. The PCR cycles were initiated at 95 °C for 5 min, followed by 35 amplification cycles. Each cycle consisted of a denaturing step at 95 °C for 30 s, an annealing step at 53 °C for 35 s, and an extension step at 72 °C for 90 s. PCR was finished with a final extension step at 72 °C for 7 min. DNA fragments were purified by 1% agarose gel purification using QIAquik Gel Extraction Kit. In this PCR, a GGGSGGG linker was also added to the 3́ end of mCherry and the 5́ end of Vm24. This linker allowed the fusion of the two genes by an overlapping PCR following the same protocol previously described, with the following exceptions: 100 ng of the amplified mCherry and Vm24 DNA were added to the reaction mix without primers. The annealing temperature was set at 69 °C, and 11 PCR cycles were run. PCR protocol was paused, and the primers F-mCherry and R-Vm24 were added to the reaction mix. The annealing temperature was readjusted to 53 °C, and the protocol was run for 23 cycles more. After the purification of the DNA products from the second PCR, DNA fragments were cloned into the yeast expression vector pPICZαA (Invitrogen, Waltham, MA, United States) using *Eco*RI and *Sal*I restriction enzymes. To construct the pPICZαA-mCherry expression vector, the mCherry sequence was amplified from the vector pmCherry-Kv1.3. The *Eco*RI and *Sal*I restriction sites were added with the forward and reverse primers, respectively (primers are shown in Table 1). PCR and cloning of the DNA fragment were performed according to the above protocols. Another important feature included in the gene cassette was the addition of the coding sequence of the 6×-HisTag at the N-terminus to facilitate protein purification by Ni-NTA affinity chromatography. The in-frame ligation and nucleotide sequences of mCherry-Vm24 and mCherry were confirmed by DNA sequencing.

Pichia Transformation

Pichia pastoris X-33 competent cells were transformed using the expression vector previously linearized by *SacI* restriction enzyme digestion at 37 °C overnight. The transformation was performed using the Pichia EasyComp Transformation Kit (Invitrogen, United States) according to the manufacturer's protocol. Transformed cells were plated on a YPD agar plate (1% yeast extract, 2% peptone, 2% dextrose, 2% agar, and pH 7.0) containing 200 μg/mL Zeocin. The 25 largest colonies after 72 h of incubation at 30 °C were grown on a YPD plate supplemented with increasing amounts of Zeocin (500, 1000, and 2000 μg/mL) to select the clone exhibiting hyper-resistance to Zeocin. Gene integration into the genome of *Pichia* transformants was confirmed by colony PCR using plasmid- and gene-specific primers.

mCherry and mCherry-Vm24 Expression and Purification

Nine selected clones from the YPD plate containing 2000 μg/mL Zeocin were cultured overnight at 30 °C at 240 rpm in 5

https://doi.org/10.1021/acsomega.5c10479
ACS Omega XXXX, XXX, XXX−XXX

mL of YPD medium (1% yeast extract, 2% peptone, 2% dextrose, pH 7.0). These cultures were then diluted in 10 mL of BMGY medium (1% yeast extract, 2% peptone, 100 mM potassium phosphate, pH 6.0, 1.34% YNB, 4×10^{-5}% biotin, and 2% glycerol) to achieve an OD_{600} = 0.2. Clones were incubated at 30 °C with constant shaking at 240 rpm for 24 h. Cells were then harvested by centrifugation, resuspended in 2 mL BMMY induction medium (similar to BMGY but containing 1% methanol instead of glycerol), and grown at 30 °C with continuous shaking at 240 rpm for 72 h. To maintain protein induction, absolute methanol was added every 24 h to a final concentration of 1%. For each sample, 1 mL of supernatant was collected and protein was precipitated using the trichloroacetic acid protocol and then analyzed on a 16% Tricine SDS-PAGE gel. The clone with the highest expression level was cultured in 100 mL BMGY (30 °C at 240 rpm for 24 h), then the cells were harvested and resuspended in 50 mL BMMY. After 72 h of protein expression induction (30 °C at 240 rpm), the cells were separated from the supernatant by high-speed centrifugation, and then the supernatant was filtered, and imidazole was added at a final concentration of 30 mM. The filtered supernatant was loaded on a Ni SepharoseTM 6 Fast Flow (Cytiva, Sweden AB) manually packed column pre-equilibrated with a binding buffer (25 mM potassium phosphate, 300 mM NaCl, 30 mM imidazole, pH 7.4) at a flow rate of 1 mL/min using a peristaltic pump (Miniplus 3, GILSON). The column was washed with three column volumes (CVs) of wash buffer (25 mM potassium phosphate, 300 mM NaCl, 40 mM imidazole, pH 7.4) and peptides were eluted by running three CVs of elution buffer (25 mM potassium phosphate, 400 mM imidazole, pH 7). The eluted sample was concentrated by an AMICON tube with a 10 kDa cutoff (Merck Millipore, Tullagreen, Ireland) and further purified by size exclusion-high-performance liquid chromatography (SE-HPLC) using a BioBasic SE-1000 column (300 × 7.8 mm, 5 μM particle size, Thermo Scientific) using a Prominence HPLC system (Shimadzu, Germany) at a flow rate of 1 mL/min in Tris 50 mM buffer pH 8. The fractions obtained from SE-HPLC were concentrated using AMICON tubes for subsequent experiments. The concentrated product was frozen at-20 °C and was repeatedly frozen and thawed without loss of the Kv1.3 inhibitory potential.

Mass Spectrometry Analysis

Mass spectrometric determinations were performed using an ESI QTOF-MS instrument (maXis II UHR ESI-QTOF MS, Bruker, Bremen, Germany). The mass spectrometer was operated in positive ionization mode; 0.5 bar nebulizer pressure, 200 °C dry gas temperature, 4 L/min dry gas flow rate, 4000 V capillary voltage, 500 V end plate offset, 1 Hz spectra rate, and 500−2,500 m/z mass range were applied. ESI tuning mix (Agilent) calibrant injected after each run enabled internal m/z calibration. Mass spectra were processed and evaluated by Compass Data Analysis version 4.4 (Bruker).

Cells

Chinese hamster ovary (CHO) cells were maintained by culturing in Dulbecco's modified Eagle's medium (DMEM, Gibco) supplemented with 2 mM L-glutamine, 10% FBS, 100 μg/mL streptomycin, and 100 U/mL penicillin-G (Sigma-Aldrich) in a humidified incubator at 37 °C and 5% CO_2. CHO cells were transiently transfected using the Lipofectamine 2000 kit (Invitrogen) according to the manufacturer's protocol. The following plasmids encoding ion channels were used for transfection: hKV1.1 (KCNA1 gene), and hKV1.2 (KCNA2 gene) in pCMV6-AC-GFP plasmid (OriGene Technologies), hKv1.3 (KCNA3 gene) in pEGFP-C1 (Clontech, USA), and hKCa3.1 (KCNN4 gene) in pEGFP-C1 plasmid (a kind gift from H. Wulff, University of California, Davis, CA). At 24 h after transfection, GFP-expressing transfectants were identified with Nikon TE 2000U fluorescence microscope (Nikon, Tokyo, Japan) using bandpass filters of 455−495 nm and 515−555 nm for excitation and emission, respectively. Human venous blood from anonymized healthy donors was obtained from a blood bank. Peripheral blood mononuclear cells (PBMCs) were isolated by density gradient centrifugation using Histopaque-1077. The obtained cells were resuspended in RPMI 1640 medium containing 10% fetal calf serum, 100 μg/mL penicillin, 100 μg/mL streptomycin, and 2 mL glutamine, seeded at a density of 5×10^5 cells per mL in a 24-well culture plate, and grown in a 5% CO_2 incubator at 37 °C for 2−5 days. Phytohemagglutinin A was added to the medium at concentrations of 7 μg/mL to increase voltage-gated potassium ion channel expression. The hKv1.3-expressing stable CHO cell line was established as previously described.[57] In brief, the cDNA encoding the wild-type hKv1.3 channel (European Nucleotide Archive accession no. M85217) tagged with GFP at the N-terminus was cloned into the pBMN-LacZ retroviral vector. This construct (GFP-hKv1.3), along with helper plasmids, was transfected into HEK-293T cells. The virus particles produced in these HEK-293T cells were then used to transduce CHO cells. The biophysical properties of this channel have been previously evaluated.[57]

Electrophysiology

Electrophysiological recordings were conducted utilizing the patch-clamp methodology in whole-cell configuration on voltage-clamped cells. The Axon Multiclamp 700B amplifier and Axon Digidata 1440 digitizer were employed to facilitate data acquisition, which was managed by Clampex 10.7 software (all sourced from Molecular Devices, Sunnyvale, CA). Micropipettes were pulled from GC150F-15 borosilicate capillaries (Harvard Apparatus Kent, United Kingdom), resulting in 3−4 MΩ resistance in the extracellular solution. For the measurement of hKv1.1, hKv1.2, and hKv1.3, the normal extracellular solution contained 145 mM NaCl, 5 mM KCl, 1 mM $MgCl_2$, 2.5 mM $CaCl_2$, 5.5 mM glucose, and 10 mM 4-(2-hydroxyethyl)-1-piperazineethanesulfonic acid (HEPES), with a pH of 7.35. The HK extracellular solution contained 150 mM K^+, and lacked Na^+, all other components were the same as in the normal extracellular solution. The extracellular solution for KCa3.1 recordings consisted of 145 mM L-aspartic acid Na^+ salt, 5 mM KCl, 2.5 mM $CaCl_2$, 1 mM $MgCl_2$, 5.5 mM glucose, and 10 mM HEPES, with a pH of 7.4. The osmolarity of the solutions ranged between 302 and 308 mOsM/L. The pipet filling solution (intracellular) for hKv1.1, hKv1.2, and hKv1.3 currents consisted of 140 mM KF, 2 mM $MgCl_2$, 1 mM $CaCl_2$, 10 mM HEPES, and 11 mM ethylene glycol-bis(2-aminoethyl ether)-*N*,*N*,*N*,*N*-tetraacetic acid (EGTA), with a pH of 7.22. The intracellular solution for KCa3.1 recording consisted of 150 mM K-Asp, 5 mM HEPES, 8.5 mM $CaCl_2$, 1 mM $MgCl_2$, 10 mM EDTA, pH 7.22. The estimated free Ca^{2+} concentration in this solution is 1 μM, calculated using the MaxChelator program (https://somapp.ucdmc.ucdavis.edu/pharmacology/bers/maxchelator/

https://doi.org/10.1021/acsomega.5c10479
ACS Omega XXXX, XXX, XXX−XXX

webmaxc/webmaxcE.htm). The measured osmolarity of intracellular solutions was ~295 mOsm/L. When mCherry-Vm24 was dissolved in an extracellular solution at different molar concentrations, it was supplemented with 0.1 mg/mL bovine serum albumin (BSA). To record hKv1.1, hKv1.2, and hKv1.3 currents, 15 to 50 ms-long depolarizing pulses were applied at +50 mV from a holding potential of −120 mV every 15 s. To record the hKCa3.1 currents, a 150 ms-long voltage ramp to +50 mV from −120 mV was applied every 10 s. Current traces were low-pass filtered by the analog four-pole Bessel filters of the amplifiers, and the sampling frequency was set at 20 kHz, at least twice that of the filter cutoff frequency. Test solutions were applied directly onto the measured cell using a gravity-driven perfusion system using an AutoMate Perfusion Pencil Multi-Barrel Manifold Tip (AutoMate Scientific, Berkeley, CA, USA). The excess bath solution was constantly removed with vacuum suction.

Patch-Clamp Data Analyses

The inhibitory effect of the mCherry-Vm24 at a specific molar concentration was determined by calculating the remaining current fraction (RCF = I/I_0), where I_0 represents the peak current in the absence of the mCherry-Vm24, and I represents the peak current at equilibrium block for a given mCherry-Vm24 concentration. When the toxin did not cause obvious inhibition of the current (e.g., in the case of hKv1.1), the I value was measured 7 min after the start of the perfusion with the toxin-containing solution. The data points on the dose−response curves reflect the average of 3−4 individual measurements. Subsequently, the data points were fitted using the Hill equation,

$$\mathrm{RCF} = \frac{K_d^H}{K_d^H + [\mathrm{Tx}]^H}$$

where [Tx] is the concentration of the mCherry-Vm24 and H is the Hill coefficient. The best-fit curve gave a K_d value for the fusion protein.

Optical Spectrophotometry

Fluorescence emission and excitation profiles of 1 μM mCherry-Vm24 were measured in phosphate-buffered saline (PBS) using a Fluorolog-3 spectrofluorometer (Horiba Jobin Yvon, Edison, NJ). The excitation spectrum was obtained through emission at 587 nm, while the emission spectrum was obtained through excitation at 610 nm. Both the excitation and emission slits were set at a width of 2 nm, and the speed of the monochromator was 150 nm/s.

Confocal Microscopy

Labeling of the hKv1.3 channel by the mCherry-Vm24 was evaluated in transfected CHO cells using confocal laser scanning microscopy as follows. 24 h after transfection, the cells were washed twice in phosphate-buffered saline (PBS) supplemented with 1% FBS and then incubated with 10 nM mCherry-Vm24 or mCherry for 1 h at 37 °C. After incubation, the cells were washed twice in PBS supplemented with 1% FBS. Fluorescent images were recorded on an LMS880 confocal laser scanning microscope (Carl Zeiss GmbH, Jena, Germany), using a 40× C-Apochromat water immersion objective (NA = 1.2, item no.: 421767-9971). Laser lines of 488 and 533 nm were used for the excitation of GFP and mCherry-Vm24, and the fluorescence emissions of GFP and mCherry-Vm24 were detected through bandpass filters of 493−591 and 581−697 nm, respectively.

Flow Cytometry

Nontransfected CHO and GFP-Kv1.3 expressing stable CHO cells were labeled with mCherry-Vm24 to study the Kv1.3 expression using flow cytometry. For each treatment, 2.5×10^5 cells were first washed twice with PBS supplemented with 2% FBS (v/v) and then stained with 10 nM of mCherry-Vm24 at room temperature in the dark for 30 min. Cells were washed with 3 mL of PBS containing 2% FBS (v/v), resuspended in 200 μL of the same buffer, and subjected to flow cytometer analysis. For the competition assay, cells were first incubated with 100 nM of recombinant Vm24 (rVm24) for 20 min and then stained with 10 nM of mCherry-Vm24 for 30 min. All the samples were analyzed on a NovoCyte 3000 RYB flow cytometer (ACEA Biosciences Inc.). The GFP and mCherry were excited with blue (488 nm) and yellow (561 nm) lasers, respectively, and the emission filters 530/30 nm and 615/20 nm were used for GFP and mCherry, respectively. 20,000 events were measured for each sample, and data were analyzed by FlowJo software vX.0.7 (Ashland, OR). In brief, live cells were gated based on their forward scatter height (FSC-H) and side scatter height (SSC-H) parameters, and histograms corresponding to mCherry-Vm24 labeling were plotted as peak-normalized overlays. The staining experiments were repeated three times independently.

Biodistribution Assay

Mice were anesthetized via inhalation of isoflurane and subsequently injected with mCherry-Vm24 diluted in PBS at a dose of 3 μg/g body weight via the tail vein. At predetermined time points, postinjection (5 min, 1 h, and 6 h), mice were euthanized with CO_2 inhalation, and major organs (liver, kidneys, lungs, spleen, heart, and brain) were harvested. The organs were imaged by an IVIS Spectrum In Vivo Imaging System (PerkinElmer, MA, USA) ex vivo to quantify the fluorescent activity specific to each organ. Fluorescence intensity was measured using the Living Image software, which was calibrated to detect mCherry fluorescence. Normalized fluorescence intensity was calculated by dividing the fluorescence intensity values at each time point by the highest value obtained for the corresponding organ across all treatments (mCherry, mCherry-Vm24, and control).

STATISTICS

Data are expressed as means ± SEM. Statistical analyses and graph plotting were executed in GraphPad Prism software (version 8.0.1).

ASSOCIATED CONTENT

Supporting Information

The Supporting Information is available free of charge at https://pubs.acs.org/doi/10.1021/acsomega.5c10479.

Figure S1: Characterization of recombinant mCherry (PDF)

AUTHOR INFORMATION

Corresponding Author

Gyorgy Panyi − *Department of Biophysics and Cell Biology, Faculty of Medicine, University of Debrecen, Debrecen H-4032, Hungary;* orcid.org/0000-0001-6227-3301; Phone: Phone:; Email: panyi@med.unideb.hu

https://doi.org/10.1021/acsomega.5c10479
ACS Omega XXXX, XXX, XXX−XXX

Authors

Jesús Borrego − *Department of Biophysics and Cell Biology, Faculty of Medicine, University of Debrecen, Debrecen H-4032, Hungary; HUN-REN-UD Cell Biology and Signaling Research Group, Debrecen H-4032, Hungary;* orcid.org/0000-0002-2783-8044

Muhammad Umair Naseem − *Department of Biophysics and Cell Biology, Faculty of Medicine, University of Debrecen, Debrecen H-4032, Hungary;* orcid.org/0000-0003-3849-6219

Amna Al Olaimi − *Department of Biophysics and Cell Biology, Faculty of Medicine, University of Debrecen, Debrecen H-4032, Hungary;* orcid.org/0009-0007-5946-8934

Eva Korpos − *Department of Biophysics and Cell Biology, Faculty of Medicine, University of Debrecen, Debrecen H-4032, Hungary; HUN-REN-UD Cell Biology and Signaling Research Group, Debrecen H-4032, Hungary;* orcid.org/0000-0002-0438-4211

Arpad Szoor − *Department of Biophysics and Cell Biology, Faculty of Medicine, University of Debrecen, Debrecen H-4032, Hungary;* orcid.org/0000-0002-3727-6129

Gyula Batta − *Department of Biophysics and Cell Biology, Faculty of Medicine, University of Debrecen, Debrecen H-4032, Hungary; Department of Genetics and Applied Microbiology, Faculty of Science of Technology, University of Debrecen, Debrecen H-4032, Hungary;* orcid.org/0000-0001-8735-6920

Complete contact information is available at: https://pubs.acs.org/10.1021/acsomega.5c10479

Author Contributions

‖J.B. and M.U.N. equally contributed.

Notes

The authors declare no competing financial interest.

■ ACKNOWLEDGMENTS

Project no. 2024-1.2.3-HU-RIZONT-2024-00099 (to G.P.) has been implemented with the support provided by the Ministry of Culture and Innovation of Hungary from the National Research, Development, and Innovation Fund, financed under the 2024-1.2.3-HU-RIZONT funding scheme. The grant from the Hungarian National Research, Development, and Innovation Office (K143071 to G.P.) is highly appreciated.

■ ABBREVIATIONS

BMGY, Buffered glycerol-complex medium; BMMY, Buffered methanol-complex medium; BSA, Bovine serum albumin; CHO, Chinese hamster ovary; CV, Column volume; DNA, Deoxyribonucleic Acid; EGTA, Ethylene glycol-bis(2-aminoethyl ether)-*N*,*N*,*N*,*N*-tetraacetic acid; ESI QTOF-MS, Electrospray ionization-quadrupole-time-of-flight-mass spectrometry; FBS, Fetal bovine serum; GFP, Green fluorescent protein; HEPES, 4-(2-hydroxyethyl)-1-piperazineethanesulfonic acid; Ni-NTA, Ni^{2+}-nitrilotriacetic acid; PBMC, Peripheral blood mononuclear cells; PBS, Phosphate-buffered saline; PCR, Polymerase chain reaction; RCF, Remaining current fraction; RFP, Red fluorescent protein; RP-HPLC, Reversed-phase high-performance liquid chromatography; rVm24, Recombinant Vm24; SDS-PAGE, Sodium dodecyl sulfate−polyacrylamide gel electrophoresis; SE-HPLC, Size exclusion−high performance liquid chromatography; SEM, Standard error of the mean; YPD, Yeast extract peptone-dextrose

■ REFERENCES

(1) Perez-Garcia, M. T.; Cidad, P.; Lopez-Lopez, J. R. The secret life of ion channels: Kv1.3 potassium channels and proliferation. *Am. J. Physiol. Cell Physiol.* **2018**, *314* (1), C27−C42.

(2) Veytia-Bucheli, J. I.; Jiménez-Vargas, J. M.; Melchy-Pérez, E. I.; Sandoval-Hernández, M. A.; Possani, L. D.; Rosenstein, Y. Kv1.3 channel blockade with the Vm24 scorpion toxin attenuates the CD4+ effector memory T cell response to TCR stimulation. *Cell Commun. Signal.* **2018**, *16* (1), 45.

(3) Wang, X.; Li, G.; Guo, J.; Zhang, Z.; Zhang, S.; Zhu, Y.; Cheng, J.; Yu, L.; Ji, Y.; Tao, J. Kv1.3 Channel as a Key Therapeutic Target for Neuroinflammatory Diseases: State of the Art and Beyond. *Front. Neurosci.* **2020**, *13*, 1393.

(4) Rangaraju, S.; et al. Kv1.3 potassium channels as a therapeutic target in multiple sclerosis. *Expert Opin. Ther. Targets* **2009**, *13* (8), 909−924.

(5) Cazaña-Pérez, V.; Cidad, P.; Navarro-González, J. F.; Rojo-Mencía, J.; Jaisser, F.; López-López, J. R.; de la Rosa, D. A.; Giraldez, T.; Pérez-García, M. T. Kv1.3 Channel Inhibition Limits Uremia-Induced Calcification In Mouse And Human Vascular Smooth Muscle. *Function* **2020**, *2* (1), zqaa036.

(6) Bobi, J.; et al. Kv1.3 blockade inhibits proliferation of vascular smooth muscle cells in vitro and intimal hyperplasia in vivo. *Transl. Res.* **2020**, *224*, 40−54.

(7) Gubič, Š.; et al. Discovery of KV1.3 ion channel inhibitors: Medicinal chemistry approaches and challenges. *Med. Res. Rev.* **2021**, *41* (4), 2423−2473.

(8) Beeton, C.; et al. A novel fluorescent toxin to detect and investigate Kv1.3 channel up-regulation in chronically activated T lymphocytes. *J. Biol. Chem.* **2003**, *278* (11), 9928−9937.

(9) Bednenko, J.; Harriman, R.; Mariën, L.; Nguyen, H. M.; Agrawal, A.; Papoyan, A.; Bisharyan, Y.; Cardarelli, J.; Cassidy-Hanley, D.; Clark, T.; et al. A multiplatform strategy for the discovery of conventional monoclonal antibodies that inhibit the voltage-gated potassium channel Kv1.3. *mAbs* **2018**, *10* (4), 636−650.

(10) Chandy, K. G.; Norton, R. S. Peptide blockers of Kv1.3 channels in T cells as therapeutics for autoimmune disease. *Curr. Opin. Chem. Biol.* **2017**, *38*, 97−107.

(11) Yoon, S.; Cheon, S. Y.; Park, S.; Lee, D.; Lee, Y.; Han, S.; Kim, M.; Koo, H.; et al. Recent advances in optical imaging through deep tissue: imaging probes and techniques. *Biomater. Res.* **2022**, *26* (1), 57.

(12) Schutz, G. J.; Pastushenko, V. P.; Gruber, H. J.; Knaus, H.-G.; Pragl, B.; Schindler, H. 3D imaging of individual ion channels in living cells at 40 nM resolution. *Single Mol.* **2000**, *1*, 25−31.

(13) Freudenthaler, G.; et al. Ultrasensitive pharmacological characterisation of the voltage-gated potassium channel K(V)1.3 studied by single-molecule fluorescence microscopy. *Histochem. Cell Biol.* **2002**, *117* (3), 197−202.

(14) Kudryashova, K. S.; et al. Fluorescent system based on bacterial expression of hybrid KcsA channels designed for Kv1.3 ligand screening and study. *Anal. Bioanal. Chem.* **2013**, *405* (7), 2379−2389.

(15) Kuzmenkov, A. I.; Nekrasova, O. V.; Kudryashova, K. S.; Peigneur, S.; Tytgat, J.; Stepanov, A. V.; Kirpichnikov, M. P.; Grishin, E. V.; Feofanov, A. V.; Vassilevski, A. A. Fluorescent protein-scorpion toxin chimera is a convenient molecular tool for studies of potassium channels. *Sci. Rep.* **2016**, *6* (1), 33314.

(16) Nekrasova, O. V.; Primak, A. L.; Ignatova, A. A.; Novoseletsky, V. N.; Geras'kina, O. V.; Kudryashova, K. S.; Yakimov, S. A.; Kirpichnikov, M. P.; Arseniev, A. S.; Feofanov, A. V.; et al. N-Terminal Tagging with GFP Enhances Selectivity of Agitoxin 2 to Kv1.3-Channel Binding Site. *Toxins* **2020**, *12* (12), 802.

(17) Primak, A. L.; et al. Kv1 Potassium Channel Ligands Based on Hongotoxin 1 and Red Fluorescent Protein. *Russ. J. Bioorg. Chem.* **2020**, *46* (6), 1011−1017.

(18) Denisova, K. R.; Orlov, N. A.; Yakimov, S. A.; Kryukova, E. A.; Dolgikh, D. A.; Kirpichnikov, M. P.; Feofanov, A. V.; Nekrasova, O. V.; et al. GFP-Margatoxin, a Genetically Encoded Fluorescent Ligand to Probe Affinity of Kv1.3 Channel Blockers. *Int. J. Mol. Sci.* **2022**, *23* (3), 1724.
(19) Giepmans, B. N.; et al. The fluorescent toolbox for assessing protein location and function. *Science* **2006**, *312* (5771), 217−224.
(20) Varga, Z.; et al. Vm24, a natural immunosuppressive peptide, potently and selectively blocks Kv1.3 potassium channels of human T cells. *Mol. Pharmacol.* **2012**, *82* (3), 372−382.
(21) Wu, B.; Chen, Y.; Muller, J. D. Fluorescence fluctuation spectroscopy of mCherry in living cells. *Biophys. J.* **2009**, *96* (6), 2391−2404.
(22) Borrego, J.; Naseem, M. U.; Sehgal, A. N. A.; Panda, L. R.; Shakeel, K.; Gaspar, A.; Nagy, C.; Varga, Z.; Panyi, G.; et al. Recombinant Expression in Pichia pastoris System of Three Potent Kv1.3 Channel Blockers: Vm24, Anuroctoxin, and Ts6. *J. Fungi.* **2022**, *8* (11), 1215.
(23) Gurrola, G. B.; et al. Structure, function, and chemical synthesis of Vaejovis mexicanus peptide 24: a novel potent blocker of Kv1.3 potassium channels of human T lymphocytes. *Biochemistry* **2012**, *51* (19), 4049−4061.
(24) Stamatas, G. N.; Southall, M.; Kollias, N. In Vivo Monitoring of Cutaneous Edema using Spectral Imaging in the Visible and Near Infrared. *J. Invest. Dermatol.* **2006**, *126* (8), 1753−1760.
(25) Stolik, S.; et al. Measurement of the penetration depths of red and near infrared light in human "ex vivo" tissues. *J. Photochem. Photobiol. B* **2000**, *57* (2−3), 90−93.
(26) Ash, C.; et al. Effect of wavelength and beam width on penetration in light-tissue interaction using computational methods. *Lasers Med. Sci.* **2017**, *32* (8), 1909−1918.
(27) Argos, P. An investigation of oligopeptides linking domains in protein tertiary structures and possible candidates for general gene fusion. *J. Mol. Biol.* **1990**, *211* (4), 943−958.
(28) Shaner, N. C.; et al. Improved monomeric red, orange and yellow fluorescent proteins derived from Discosoma sp. red fluorescent protein. *Nat. Biotechnol.* **2004**, *22* (12), 1567−1572.
(29) Day, R. N.; Davidson, M. W. The fluorescent protein palette: tools for cellular imaging. *Chem. Soc. Rev.* **2009**, *38* (10), 2887−2921.
(30) Doherty, G. P.; Bailey, K.; Lewis, P. J. Stage-specific fluorescence intensity of GFP and mCherry during sporulation In Bacillus Subtilis. *BMC Res. Notes* **2010**, *3*, 303.
(31) Hong, P.; Koza, S.; Bouvier, E. S. Size-Exclusion Chromatography for the Analysis of Protein Biotherapeutics and their Aggregates. *J. Liq. Chromatogr. Relat. Technol.* **2012**, *35* (20), 2923−2950.
(32) Jing, Y.; et al. Identification of cell culture conditions to control protein aggregation of IgG fusion proteins expressed in Chinese hamster ovary cells. *Process Biochem.* **2012**, *47* (1), 69−75.
(33) Koschak, A.; et al. Subunit composition of brain voltage-gated potassium channels determined by hongotoxin-1, a novel peptide derived from Centruroides limbatus venom. *J. Biol. Chem.* **1998**, *273* (5), 2639−2644.
(34) Bartok, A.; Panyi, G.; Varga, Z. Potassium Channel Blocking Peptide Toxins from Scorpion Venom. In *Scorpion Venoms*, Gopalakrishnakone, P.; Possani, L. D.; Schwartz, E. F.; de la Vega, R. C. R., Eds.; Springer: Netherlands, Dordrecht, 2015; pp. 493−527.
(35) Banerjee, A.; Lee, A.; Campbell, E.; MacKinnon, R. Structure Of a Pore-Blocking Toxin In Complex With a Eukaryotic Voltage-Dependent K+ Channel. *eLife* **2013**, *2*, No. e00594.
(36) Park, C. S.; Miller, C. Mapping function to structure in a channel-blocking peptide: electrostatic mutants of charybdotoxin. *Biochemistry* **1992**, *31* (34), 7749−7755.
(37) Catacuzzeno, L.; Fioretti, B.; Franciolini, F. Expression and Role of the Intermediate-Conductance Calcium-Activated Potassium Channel KCa3.1 in Glioblastoma. *J. Signal Transduction* **2012**, *2012*, 421564.
(38) Heike, W.; Kolski-Andreaco, A.; Sankaranarayanan, A.; Sabatier, J.-M.; Shakkottai, V. Modulators of Small- and Intermediate-Conductance Calcium-Activated Potassium Channels and their Therapeutic Indications. *Curr. Med. Chem.* **2007**, *14* (13), 1437−1457.
(39) Naseem, M. U.; Gurrola-Briones, G.; Romero-Imbachi, M. R.; Borrego, J.; Carcamo-Noriega, E.; Beltrán-Vidal, J.; Zamudio, F. Z.; Shakeel, K.; Possani, L. D.; Panyi, G. Characterization and Chemical Synthesis of Cm39 (α-KTx 4.8): a Scorpion Toxin That Inhibits Voltage-Gated K(+) Channel K(V)1.2 and Small- and Intermediate-Conductance Ca(2+)-Activated K(+) Channels K(Ca)2.2 and K(Ca)3.1. *Toxins* **2023**, *15* (1), 41.
(40) Naseem, M. U.; Carcamo-Noriega, E.; Beltrán-Vidal, J.; Borrego, J.; Szanto, T. G.; Zamudio, F. Z.; Delgado-Prudencio, G.; Possani, L. D.; Panyi, G.; et al. Cm28, a scorpion toxin having a unique primary structure, inhibits KV1.2 and KV1.3 with high affinity. *J. Gen. Physiol.* **2022**, *154* (8), No. e202213146.
(41) Shakeel, K.; Naseem, M. U.; Olamendi-Portugal, T.; Zamudio, F. Z.; Possani, L. D.; Panyi, G.; et al. Cvill6 and Cvill7: Potent and Selective Peptide Blockers of Kv1.2 Ion Channel Isolated from Mexican Scorpion Centruroides villegasi. *Toxins* **2025**, *17* (6), 279.
(42) Wai, D. C. C.; et al. A Fluorescent Peptide Toxin for Selective Visualization of the Voltage-Gated Potassium Channel KV1.3. *Bioconjugate Chem.* **2022**, *33* (11), 2197−2212.
(43) Gao, T.; Raza, S. A.; Ramesha, S.; Nwabueze, N. V.; Tomkins, A. J.; Cheng, L.; Xiao, H.; Yepes, M.; Rangaraju, S.; et al. Temporal profiling of Kv1.3 channel expression in brain mononuclear phagocytes following ischemic stroke. *J. Neuroinflammation* **2019**, *16* (1), 116.
(44) Wulff, H.; et al. The voltage-gated Kv1.3 K + channel in effector memory T cells as new target for MS. *J.Clin. Invest.* **2003**, *111* (11), 1703−1713.
(45) Beeton, C.; Wulff, H.; Standifer, N. E.; Azam, P.; Mullen, K. M.; Pennington, M. W.; Kolski-Andreaco, A.; Wei, E.; Grino, A.; Counts, D. R.; et al. Kv1.3 channels are a therapeutic target for T cell-mediated autoimmune diseases. *Proc. Natl. Acad. Sci. U. S. A.* **2006**, *103* (46), 17414−17419.
(46) Markakis, I.; et al. Kv1.3 Channel Up-Regulation in Peripheral Blood T Lymphocytes of Patients With Multiple Sclerosis. *Front. Pharmacol.* **2021**, *12*, 714841.
(47) Teisseyre, A.; Palko-Labuz, A.; Sroda-Pomianek, K.; Michalak, K. Voltage-Gated Potassium Channel Kv1.3 as a Target in Therapy of Cancer. *Front. Oncol.* **2019**, *9*, 933.
(48) Ford, W. L. The Kinetics Of Lymphocyte Recirculation Within The Rat Spleen. *Cell Prolif.* **1969**, *2* (3), 171−191.
(49) Pabst, R.; Trepel, F. The predominant role of the spleen in lymphocyte recirculation. I. Homing of lymphocytes to and release from the isolated perfused pig spleen. *Cell Tissue Kinet.* **1975**, *8* (6), 529−541.
(50) McDaniel, M. M.; Ganusov, V. V. Estimating Residence Times of Lymphocytes in Ovine Lymph Nodes. *Front. Immunol.* **2019**, *10*, 1492.
(51) Hammond, B. J. A compartmental analysis of circulatory lymphocytes in the spleen. Cell Tissue Kinet. *Cell Proliferation* **1975**, *8* (2), 153−169.
(52) Kuna, M.; Mahdi, F.; Chade, A. R.; Bidwell, G. L., III Molecular Size Modulates Pharmacokinetics, Biodistribution, and Renal Deposition of the Drug Delivery Biopolymer Elastin-like Polypeptide. *Sci. Rep.* **2018**, *8* (1), 7923.
(53) Datta-Mannan, A. Mechanisms Influencing the Pharmacokinetics and Disposition of Monoclonal Antibodies and Peptides. *Drug Metab. Dispos.* **2019**, *47* (10), 1100−1110.
(54) Lázaro-Ibáñez, E.; et al. Selection of Fluorescent, Bioluminescent, and Radioactive Tracers to Accurately Reflect Extracellular Vesicle Biodistribution in Vivo. *ACS Nano* **2021**, *15* (2), 3212−3227.
(55) Kobayashi, H.; et al. Evaluation of the in vivo biodistribution of indium-111 and yttrium-88 labeled dendrimer-1B4M-DTPA and its conjugation with anti-Tac monoclonal antibody. *Bioconjugate Chem.* **1999**, *10* (1), 103−111.
(56) Voros, O.; Szilagyi, O.; Balajthy, A.; Somodi, S.; Panyi, G.; Hajdu, P. The C-terminal HRET sequence of Kv1.3 regulates gating

https://doi.org/10.1021/acsomega.5c10479
ACS Omega XXXX, XXX, XXX−XXX

rather than targeting of Kv1.3 to the plasma membrane. *Sci. Rep.* **2018**, *8* (1), 5937.
(57) Szilágyi, O.; et al. The role of PSD-95 in the rearrangement of Kv1.3 channels to the immunological synapse. *Pflügers Archiv - Eur. J. Physiol.* **2013**, *465* (9), 1341−1353.

https://doi.org/10.1021/acsomega.5c10479
ACS Omega XXXX, XXX, XXX−XXX